

Charmless three-body decays of b -hadrons

THOMAS LATHAM¹

*Department of Physics, University of Warwick,
Coventry, CV4 7AL, United Kingdom*

A review of recent results from LHCb and the B -factories on the charmless decays of b -hadrons into three-body final states is presented.

PRESENTED AT

DPF 2013

The Meeting of the American Physical Society
Division of Particles and Fields
Santa Cruz, California, August 13–17, 2013

¹On behalf of the LHCb collaboration.

1 Introduction

Charmless decays of b -hadrons can proceed through both $b \rightarrow u$ tree and $b \rightarrow s, d$ loop (penguin) diagrams, which can interfere. Since they have a relative weak phase of γ and the diagrams appear at similar orders, this can give rise to large direct CP violation. In the decays of neutral B mesons, time-dependent analyses allow measurements of mixing-induced CP asymmetries. Comparing the values of these asymmetries with those measured in tree-dominated decays such as $B^0 \rightarrow J/\psi K_S^0$ or $B_s^0 \rightarrow J/\psi \phi$ can be a sensitive test of the Standard Model (SM), with significant deviations being a sign that new physics particles could be appearing in the loops.

Recent results from LHCb for the direct CP asymmetries, defined as

$$\mathcal{A}^{CP}(B \rightarrow f) = \frac{\Gamma(\bar{B} \rightarrow \bar{f}) - \Gamma(B \rightarrow f)}{\Gamma(\bar{B} \rightarrow \bar{f}) + \Gamma(B \rightarrow f)}, \quad (1)$$

of the decays $B^0 \rightarrow K^+\pi^-$ and $B_s^0 \rightarrow K^-\pi^+$ [1] exhibit large central values*

$$\begin{aligned} \mathcal{A}^{CP}(B_s^0 \rightarrow \pi^+ K^-) &= 0.27 \pm 0.04 \text{ (stat)} \pm 0.01 \text{ (syst)}, \\ \mathcal{A}^{CP}(B^0 \rightarrow K^+ \pi^-) &= -0.080 \pm 0.007 \text{ (stat)} \pm 0.003 \text{ (syst)}. \end{aligned}$$

The first of these constitutes the first observation of CP violation in the B_s^0 system with a significance of 6.5σ , while the latter is the world's most precise single measurement of that quantity. Combining these results with related quantities in the expression

$$\Delta \equiv \frac{\mathcal{A}^{CP}(B^0 \rightarrow K^+\pi^-)}{\mathcal{A}^{CP}(B_s^0 \rightarrow \pi^+K^-)} + \frac{\mathcal{B}(B_s^0 \rightarrow \pi^+K^-) \tau_{B^0}}{\mathcal{B}(B^0 \rightarrow K^+\pi^-) \tau_{B_s^0}} = -0.02 \pm 0.05 \pm 0.04,$$

it is found that everything is consistent with the SM expectation ($\Delta = 0$) [2].

It is necessary to form such a combination of quantities in order to test for compatibility, or otherwise, with the SM because the source of the strong phase difference is not well understood in two-body decays. Three-body decays, on the other hand, allow direct measurements of the relative strong phases through an amplitude analysis of the Dalitz plot. Determining both the magnitudes and the phases of the intermediate states provides greater information for constraining theoretical models. In addition, modelling the interferences can help to resolve trigonometric ambiguities in the measurement of weak phases, see for example Ref. [3].

2 Direct CP violation in $B^+ \rightarrow h^+ h^+ h^-$ decays

Searches for direct CP violation in $B^+ \rightarrow h^+ h^+ h^-$ decays, where $h = \pi, K$ are motivated both by the large asymmetries seen in $B \rightarrow K\pi$ decays and B -factory results

*The inclusion of charge conjugate processes is implied throughout, except in \mathcal{A}^{CP} definitions.

that have shown evidence for direct CP asymmetries in $B^+ \rightarrow \rho^0(770)K^+$ [4, 5] and $B^+ \rightarrow \phi(1020)K^+$ [6]. The recent LHCb analysis of $B^+ \rightarrow K^+h^+h^-$ decays makes measurements of the global CP asymmetry as well as the local asymmetries in regions of the Dalitz-plot.

The analysis, full details of which can be found in Ref. [7], uses the 1.0 fb^{-1} of pp collision data collected during 2011 by the LHCb detector [8]. The raw asymmetry of measured yields

$$\mathcal{A}_{\text{RAW}}^{CP} = \frac{N_{B^-} - N_{B^+}}{N_{B^-} + N_{B^+}} \quad (2)$$

is determined from a simultaneous fit to the sample of B^+ and B^- candidates. The raw asymmetry must be corrected for both production and detection asymmetries

$$\mathcal{A}^{CP} = \mathcal{A}_{\text{RAW}}^{CP} - \mathcal{A}_P(B^\pm) - \mathcal{A}_D(K^\pm), \quad (3)$$

which are determined from the control channel $B^+ \rightarrow J/\psi K^+$, where J/ψ decays to $\mu^+\mu^-$, according to the relation

$$\mathcal{A}_D(K^\pm) + \mathcal{A}_P(B^\pm) = \mathcal{A}_{\text{RAW}}^{CP}(J/\psi K^+) - \mathcal{A}^{CP}(J/\psi K^+). \quad (4)$$

This channel is well suited for this role due to its similar topology to the signal channel and since its CP asymmetry is consistent with zero and precisely determined, $\mathcal{A}^{CP}(J/\psi K^+) = (0.1 \pm 0.7)\%$ [9].

The results of the fit to the data sample are shown in Figure 1 and the values of the CP asymmetries are found to be

$$\begin{aligned} \mathcal{A}^{CP}(B^+ \rightarrow K^+\pi^+\pi^-) &= 0.032 \pm 0.008 (\text{stat}) \pm 0.004 (\text{syst}) \pm 0.007 (J/\psi K^+), \\ \mathcal{A}^{CP}(B^+ \rightarrow K^+K^+K^-) &= -0.043 \pm 0.009 (\text{stat}) \pm 0.003 (\text{syst}) \pm 0.007 (J/\psi K^+). \end{aligned}$$

The significance of CP violation in each decay mode is 2.8σ and 3.7σ , respectively.

The variation of the raw asymmetry over the Dalitz plot is also studied and the results are shown in Figure 2. In some regions there are extremely large asymmetries present, in particular around the ρ^0 resonance in $B^+ \rightarrow K^+\pi^+\pi^-$ but also in regions that are not clearly associated with a resonance. The local CP asymmetries in the region where $m_{K^+\pi^-}^2 < 15 (\text{GeV}/c^2)^2$ and $0.08 < m_{\pi^+\pi^-}^2 < 0.66 (\text{GeV}/c^2)^2$ in $B^+ \rightarrow K^+\pi^+\pi^-$ and in the region $m_{K^+K^-}^2 < 15 (\text{GeV}/c^2)^2$ and $1.2 < m_{K^+K^-}^2 < 2.0 (\text{GeV}/c^2)^2$ are determined to be

$$\begin{aligned} \mathcal{A}_{\text{local}}^{CP}(B^+ \rightarrow K^+\pi^+\pi^-) &= 0.678 \pm 0.078 (\text{stat}) \pm 0.032 (\text{syst}) \pm 0.007 (J/\psi K^+), \\ \mathcal{A}_{\text{local}}^{CP}(B^+ \rightarrow K^+K^+K^-) &= -0.226 \pm 0.020 (\text{stat}) \pm 0.004 (\text{syst}) \pm 0.007 (J/\psi K^+), \end{aligned}$$

respectively.

The BaBar experiment has recently made an update of their analysis of $B^+ \rightarrow K^+K^+K^-$, in order to provide a direct comparison with the LHCb results for the

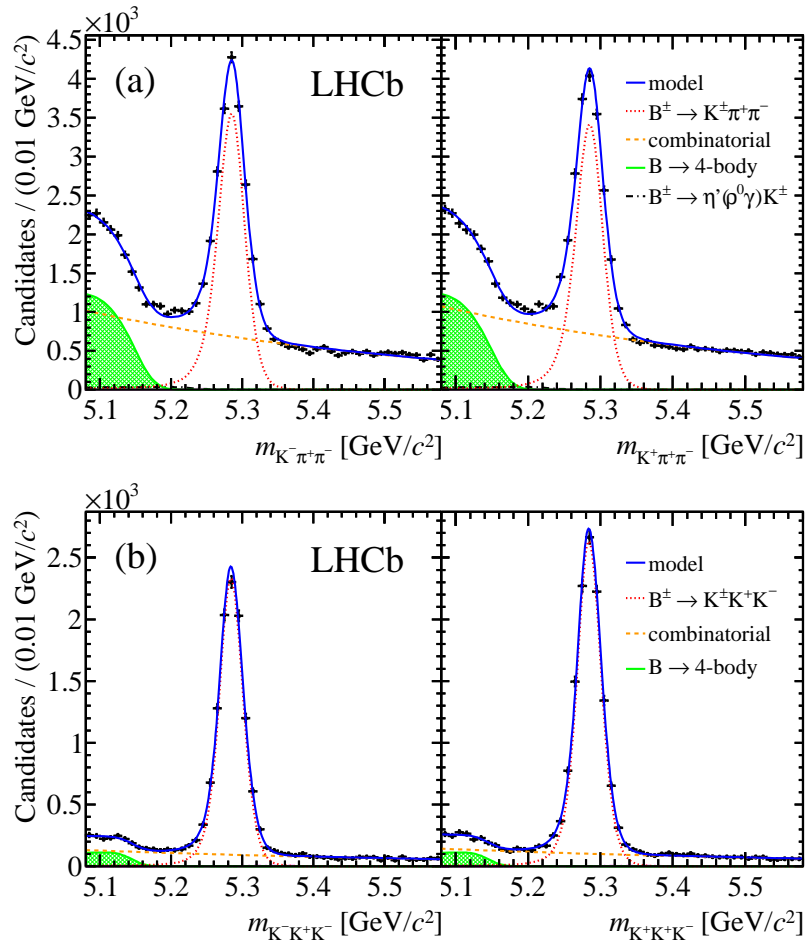


Figure 1: Distributions of the B -candidate invariant mass for (a) $B^+ \rightarrow K^+ \pi^+ \pi^-$ decays and (b) $B^+ \rightarrow K^+ K^+ K^-$ decays. The left (right) plots show the B^- (B^+) decays.

asymmetry as a function of $m_{K^+ K^-}$ [10]. This comparison is shown in Figure 3. The shapes of the distributions are extremely similar, albeit with a small offset, which is determined to be 0.045 ± 0.021 (0.053 ± 0.021) for the $m_{K^+ K^-}^2$ -low ($m_{K^+ K^-}^2$ -high) spectrum. However, it must be remembered that the LHCb distribution is that of the raw asymmetry and hence has not been corrected for production and detection effects. These are of the order of 1% and act in the direction to decrease the mild discrepancy.

Very similar findings to those from $B^+ \rightarrow K^+ h^+ h^-$ decays are made in a preliminary analysis of $B^+ \rightarrow \pi^+ \pi^+ \pi^-$ and $B^+ \rightarrow \pi^+ K^+ K^-$ [11], both in terms of the large local asymmetries and the opposite sign of the asymmetries between the two modes. In addition, the local asymmetries are observed mainly in regions not clearly

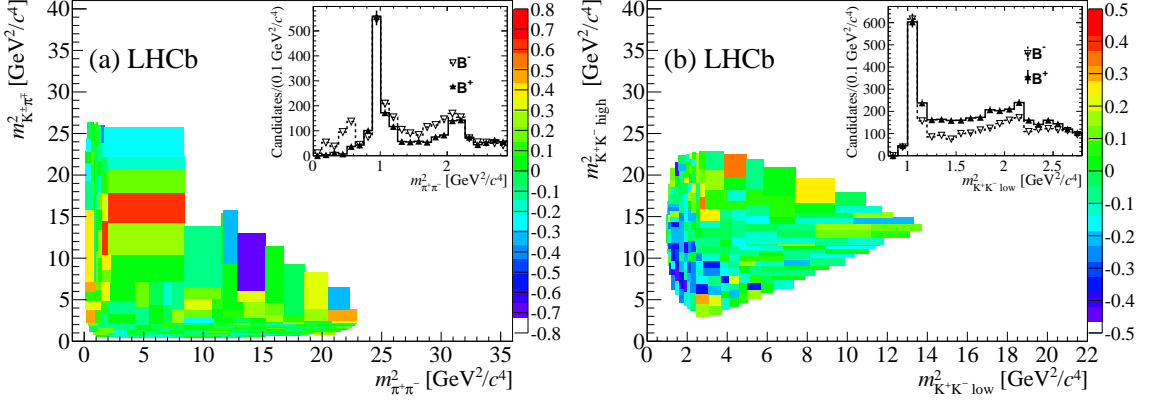


Figure 2: Variation of the raw asymmetry over the Dalitz plot in (a) $B^+ \rightarrow K^+ \pi^+ \pi^-$ and (b) $B^+ \rightarrow K^+ K^+ K^-$ decays.

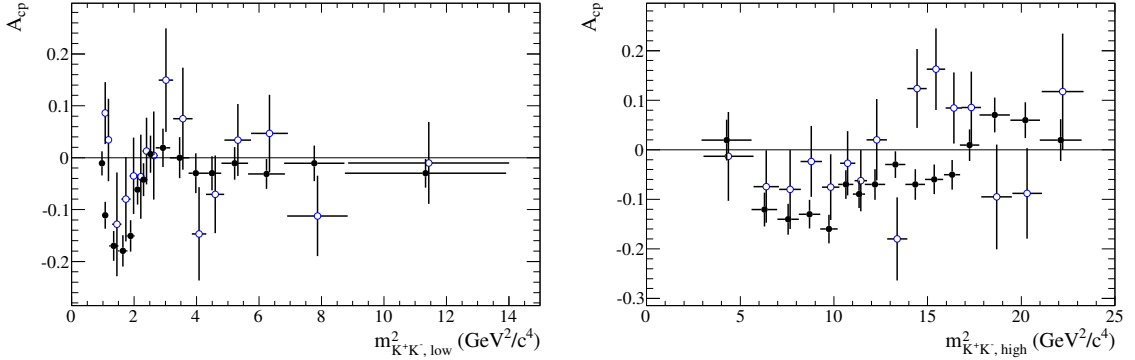


Figure 3: Asymmetry as a function of (left) $m^2_{K^+ K^- \text{ low}}$ (right) $m^2_{K^+ K^- \text{ high}}$ for $B^+ \rightarrow K^+ K^+ K^-$ decays. The BaBar (LHCb) data are the open (filled) circles.

associated with a well established resonance. This could indicate that $\pi^+ \pi^- \rightarrow K^+ K^-$ rescattering is playing a role in the generation of the strong phase difference. Amplitude analyses of these modes using the larger dataset now available at LHCb (3 fb^{-1}) will provide more information to resolve this puzzle.

3 Dynamics of $B^+ \rightarrow p \bar{p} h^+$ decays

The large asymmetries seen in $B^+ \rightarrow h^+ h^+ h^-$ decays raise the question about the role of $\pi^+ \pi^- \leftrightarrow K^+ K^-$ rescattering in these modes. The closely related decays $B^+ \rightarrow p \bar{p} h^+$ can shed some light on this issue since it is expected that $h^+ h^- \leftrightarrow p \bar{p}$ rescattering should be much smaller. The threshold enhancements seen in many $B \rightarrow p \bar{p} X$ decays provide further motivation for studying these decays. The analysis, which uses the

LHCb 1.0fb^{-1} data sample collected during 2011, studies the dynamics of the decays as well as the CP asymmetries. Full details can be found in Ref. [12].

Fits to the B -candidate invariant mass distribution, shown in Figure 4, yield 7029 ± 139 (656 ± 70) signal events for the mode $B^+ \rightarrow p\bar{p}K^+$ ($B^+ \rightarrow p\bar{p}\pi^+$), where the uncertainties are statistical only. The fit model contains contributions from signal, cross-feed (where the kaon in the signal mode is mis-identified as a pion or vice versa), combinatorial and partially-reconstructed backgrounds. The CP asymmetries for $B^+ \rightarrow p\bar{p}K^+$ are determined by repeating the fits to the B -candidate invariant mass in bins of both the $p\bar{p}$ and $K^+\bar{p}$ invariant masses and separating by the charge of the B candidate. The results are shown in Figure 5 and are consistent with zero in all bins, albeit with large uncertainties.

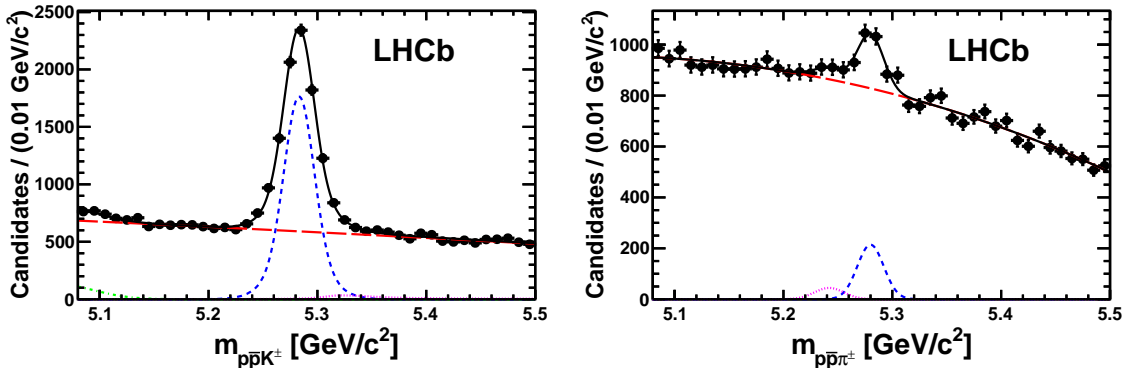


Figure 4: Distributions of the B -candidate invariant mass for (left) $B^+ \rightarrow p\bar{p}K^+$ decays and (right) $B^+ \rightarrow p\bar{p}\pi^+$ decays.

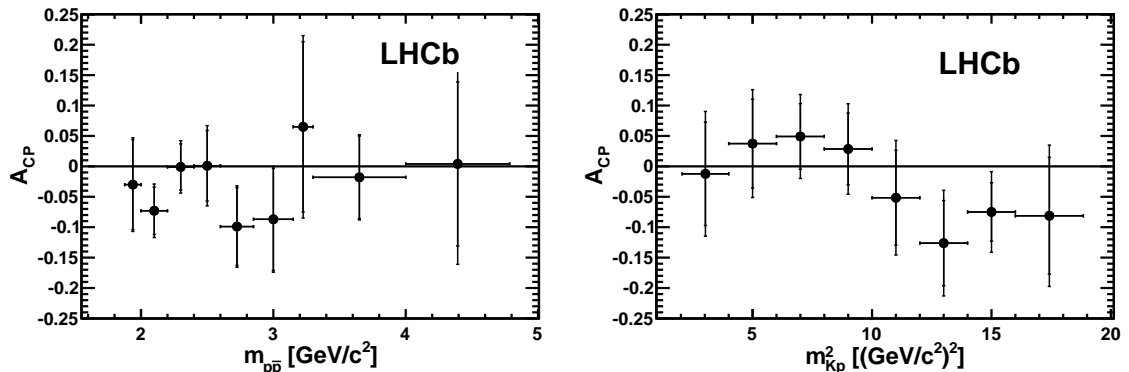


Figure 5: CP asymmetry as a function of (left) $m_{p\bar{p}}$ (right) $m_{K^+\bar{p}}$ for $B^+ \rightarrow p\bar{p}K^+$ decays.

The decay dynamics are studied by constructing differential production spectra

as a function of the invariant masses and the cosine of the angle, θ_p , between the daughter meson and the opposite-sign baryon in the $p\bar{p}$ rest frame. The distributions as a function of $p\bar{p}$ invariant mass are shown in Figure 6 and show very clear threshold enhancement behaviour, similar to other $B \rightarrow p\bar{p}X$ decays. The distributions as a function of $\cos\theta_p$ are shown in Figure 7 and exhibit strikingly opposite behaviour between the two decay modes, the forward/backward asymmetries being

$$\begin{aligned} A_{\text{FB}}(B^+ \rightarrow p\bar{p}K^+) &= 0.370 \pm 0.018 (\text{stat}) \pm 0.016 (\text{syst}), \\ A_{\text{FB}}(B^+ \rightarrow p\bar{p}\pi^+) &= -0.392 \pm 0.117 (\text{stat}) \pm 0.015 (\text{syst}). \end{aligned}$$

This behaviour can also clearly be seen when examining the $B^+ \rightarrow p\bar{p}K^+$ Dalitz plot shown in Figure 8, which has been background-subtracted using the *sPlot* technique [13]. The other clear features are the vertical bands at high $p\bar{p}$ invariant mass, which are contributions from charmonium intermediate states. These have been studied separately in an analysis reported in Ref. [14]. There is also some structure at low $m_{K^+\bar{p}}$, which is shown more clearly in the signal *sPlot* invariant mass projection in Figure 9. A two-dimensional fit to the B -candidate invariant mass and $m_{K^+\bar{p}}$ is performed in this region in order to extract the yield of the $\bar{\Lambda}(1520)$ resonance. The signal is found to have a significance of 5.1σ , which constitutes first observation of the decay $B^+ \rightarrow \bar{\Lambda}(1520)p$ with a branching fraction of

$$\mathcal{B}(B^+ \rightarrow \bar{\Lambda}(1520)p) = (3.9^{+1.0}_{-0.9} (\text{stat}) \pm 0.1 (\text{syst}) \pm 0.3(\text{BF})) \times 10^{-7},$$

where the third uncertainty is from the branching fraction of $B^+ \rightarrow J/\psi K^+$, $J/\psi \rightarrow p\bar{p}$.

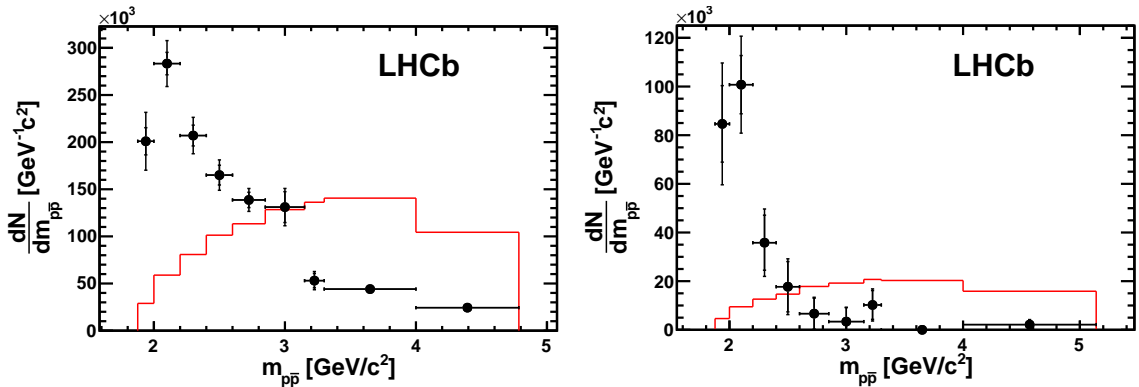


Figure 6: Differential production spectra as a function of $m_{p\bar{p}}$ for (left) $B^+ \rightarrow p\bar{p}K^+$ decays (right) $B^+ \rightarrow p\bar{p}\pi^+$ decays.

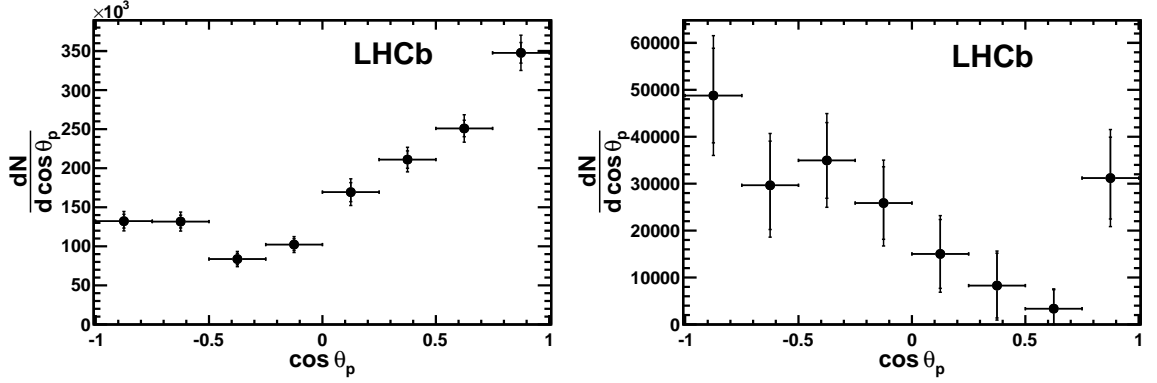


Figure 7: Differential production spectra as a function of $\cos \theta_p$ for (left) $B^+ \rightarrow p\bar{p}K^+$ decays (right) $B^+ \rightarrow p\bar{p}\pi^+$ decays.

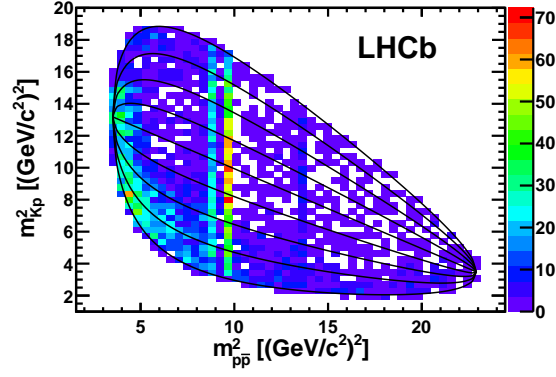


Figure 8: Dalitz plot distribution for $B^+ \rightarrow p\bar{p}K^+$ signal events. The black solid curves are lines of constant $\cos \theta_p$.

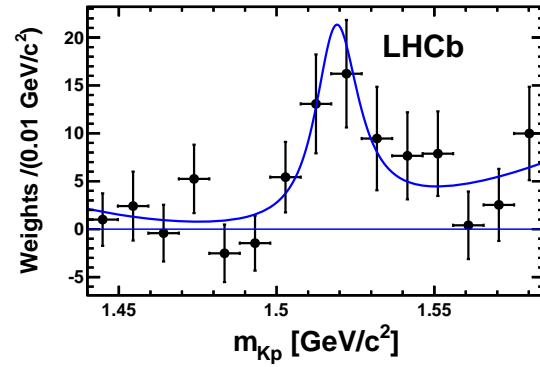


Figure 9: Distribution of $K^+\bar{p}$ invariant mass for $B^+ \rightarrow p\bar{p}K^+$ signal events in the region $1.440 < m_{K^+\bar{p}} < 1.585 \text{ GeV}/c^2$.

4 Results from $B^0 \rightarrow h^+ h^- \pi^0$ decays

The Belle collaboration have recently reported the results of a search for the decay $B^0 \rightarrow K^+ K^- \pi^0$, using a data sample of 772 million $B\bar{B}$ pairs. Full details of the analysis are given in Ref. [15]. A fit is performed to ΔE , the difference between the energy of the B candidate and the beam energy, and the output of a neural network of event-shape variables. The latter variable is a powerful discriminant against the dominant background from continuum light-quark production. The fit yields 299 ± 83 signal events, where the uncertainty is statistical only. The projections of the fit are shown in Figure 10. The signal has a significance of 3.5σ , which constitutes the first evidence of this decay, with a branching fraction of

$$\mathcal{B}(B^0 \rightarrow K^+ K^- \pi^0) = (2.17 \pm 0.60 (\text{stat}) \pm 0.24 (\text{syst})) \times 10^{-6}. \quad (5)$$

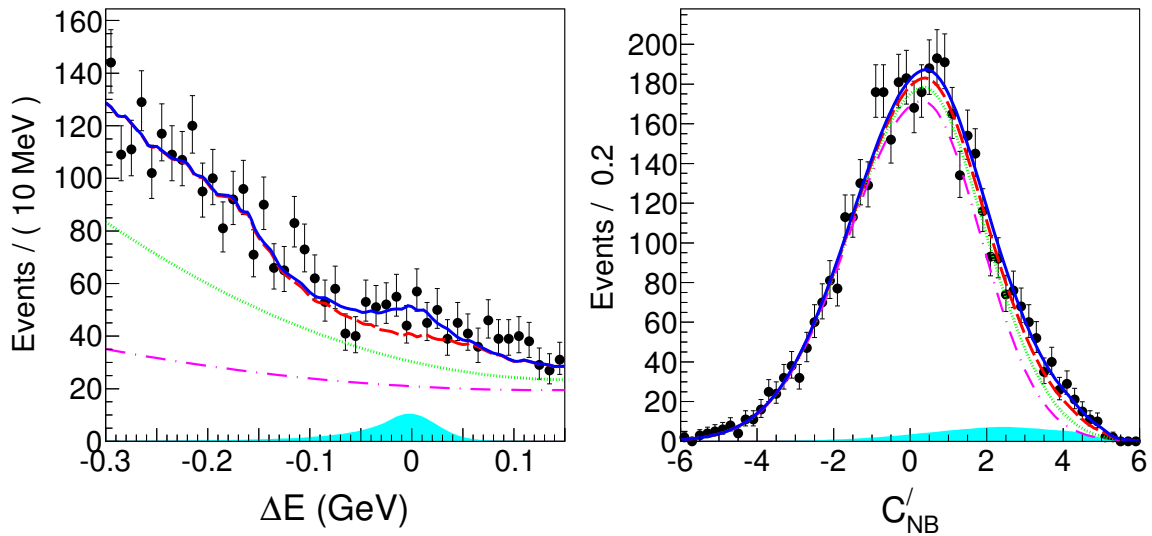


Figure 10: Projections of the maximum likelihood fit to $B^0 \rightarrow K^+ K^- \pi^0$ candidate events for the variables (left) ΔE and (right) the neural network of event-shape variables.

The BaBar collaboration have recently updated their time-dependent Dalitz-plot analysis of the decay $B^0 \rightarrow \pi^+ \pi^- \pi^0$ to use their full $\Upsilon(4S)$ dataset of 471 million $B\bar{B}$ pairs. The primary goal of this analysis is to measure the CKM angle α using the Snyder-Quinn method [16]. Full details of the analysis can be found in Ref. [17]. A thorough robustness study was conducted, which showed that while the extraction of the fit parameters and most of the derived quasi-two-body parameters was robust, unfortunately the extraction of α itself was not. However, hints of direct CP violation

were seen in the two parameters

$$A_{\rho\pi}^{+-} = \frac{\Gamma(\bar{B}^0 \rightarrow \rho^- \pi^+) - \Gamma(B^0 \rightarrow \rho^+ \pi^-)}{\Gamma(\bar{B}^0 \rightarrow \rho^- \pi^+) + \Gamma(B^0 \rightarrow \rho^+ \pi^-)}, \quad (6)$$

$$A_{\rho\pi}^{-+} = \frac{\Gamma(\bar{B}^0 \rightarrow \rho^+ \pi^-) - \Gamma(B^0 \rightarrow \rho^- \pi^+)}{\Gamma(\bar{B}^0 \rightarrow \rho^+ \pi^-) + \Gamma(B^0 \rightarrow \rho^- \pi^+)}. \quad (7)$$

The result of the 2D scan for these parameters is shown in Figure 11. The consistency with the no direct CP violation point is quantified as $\Delta\chi^2 = 6.42$.

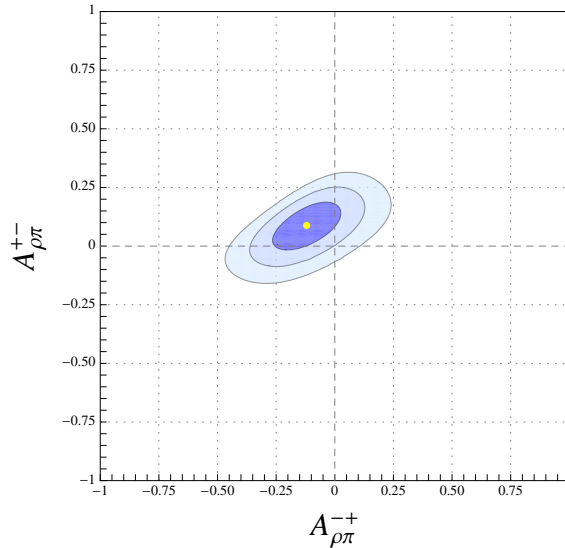


Figure 11: Likelihood scan in the $A_{\rho\pi}^{+-}$ vs. $A_{\rho\pi}^{-+}$ plane.

5 Studies of $B_{(s)}^0 \rightarrow K_S^0 h^+ h^-$ decays

Time-dependent flavour-tagged Dalitz-plot analyses of B decays to $K_S^0 h^+ h^-$ final states are sensitive to mixing-induced CP -violating phases. For example, the recent BaBar measurement $\beta_{\text{eff}}(\phi K_S^0) = (21 \pm 6 \pm 2)^\circ$ in the decay $B^0 \rightarrow K_S^0 K^+ K^-$ [6]. Such an analysis is not possible with the current LHCb statistics, however it is possible to search for the previously unobserved B_s^0 decays to these final states.

The analysis, which uses the LHCb 1.0 fb^{-1} data sample collected during 2011, has separate optimisations of the selection for the suppressed and favoured decays in each final state. In addition, most of the reconstructed K_S^0 mesons decay downstream of the LHCb Vertex Locator and so do not have information from that subdetector, while the remaining $\sim \frac{1}{3}$ do have such information. This leads to rather different

efficiencies for the two types of K_s^0 candidates (referred to as Downstream and Long, respectively) and hence the need to treat each category separately in the analysis. Full details of the analysis can be found in Ref. [18].

Figures 12 and 13 show the results of the fits to the $B_{(s)}^0 \rightarrow K_s^0 h^+ h^-$ candidate events when the selection is applied for the favoured modes and suppressed modes, respectively. The decay $B_s^0 \rightarrow K_s^0 K^\pm \pi^\mp$ is unambiguously observed and the BaBar observation of $B^0 \rightarrow K_s^0 K^\pm \pi^\mp$ [19] is confirmed. The decay $B_s^0 \rightarrow K_s^0 \pi^+ \pi^-$ is observed for the first time with a significance of 5.9σ , while no significant evidence is obtained for the decay $B_s^0 \rightarrow K_s^0 K^+ K^-$.

The branching fractions of all the modes are measured with respect to $B^0 \rightarrow K_s^0 \pi^+ \pi^-$, for which the world average branching fraction is $(2.48 \pm 0.10) \times 10^{-5}$ [9]. The ratios of branching fractions are determined to be

$$\begin{aligned}
\frac{\mathcal{B}(B^0 \rightarrow K_s^0 K^\pm \pi^\mp)}{\mathcal{B}(B^0 \rightarrow K_s^0 \pi^+ \pi^-)} &= 0.128 \pm 0.017 \text{ (stat.)} \pm 0.009 \text{ (syst.)}, \\
\frac{\mathcal{B}(B^0 \rightarrow K_s^0 K^+ K^-)}{\mathcal{B}(B^0 \rightarrow K_s^0 \pi^+ \pi^-)} &= 0.385 \pm 0.031 \text{ (stat.)} \pm 0.023 \text{ (syst.)}, \\
\frac{\mathcal{B}(B_s^0 \rightarrow K_s^0 \pi^+ \pi^-)}{\mathcal{B}(B^0 \rightarrow K_s^0 \pi^+ \pi^-)} &= 0.29 \pm 0.06 \text{ (stat.)} \pm 0.03 \text{ (syst.)} \pm 0.02 \text{ (} f_s/f_d \text{)}, \\
\frac{\mathcal{B}(B_s^0 \rightarrow K_s^0 K^\pm \pi^\mp)}{\mathcal{B}(B^0 \rightarrow K_s^0 \pi^+ \pi^-)} &= 1.48 \pm 0.12 \text{ (stat.)} \pm 0.08 \text{ (syst.)} \pm 0.12 \text{ (} f_s/f_d \text{)}, \\
\frac{\mathcal{B}(B_s^0 \rightarrow K_s^0 K^+ K^-)}{\mathcal{B}(B^0 \rightarrow K_s^0 \pi^+ \pi^-)} &\in [0.004; 0.068] \text{ at } 90\% \text{ CL},
\end{aligned}$$

where f_s/f_d refers to the uncertainty on the ratio of hadronisation fractions of the b quark to B_s^0 and B^0 mesons [20].

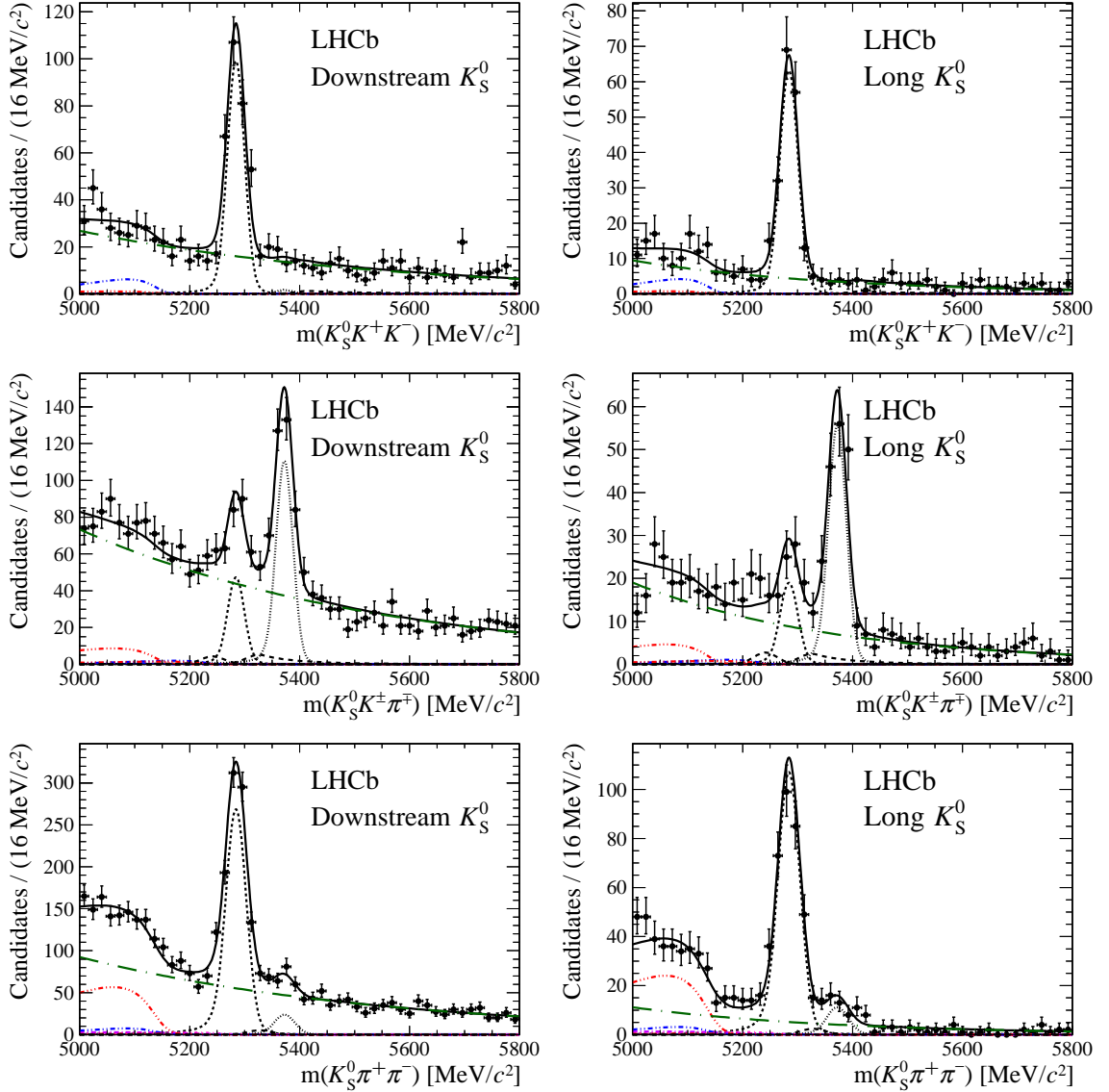


Figure 12: Invariant mass distributions of (top) $K_S^0 K^+ K^-$, (middle) $K_S^0 K^\pm \pi^\mp$, and (bottom) $K_S^0 \pi^+ \pi^-$ candidate events, with the loose selection for (left) Downstream and (right) Long K_S^0 reconstruction categories. In each plot, the total fit model is overlaid (solid black line) on the data points. The signal components are the black short-dashed or dotted lines, while cross-feed decays are the black dashed lines close to the signal peaks. The combinatorial background contribution is the green long-dash dotted line. Partially reconstructed contributions from various sources are also shown.

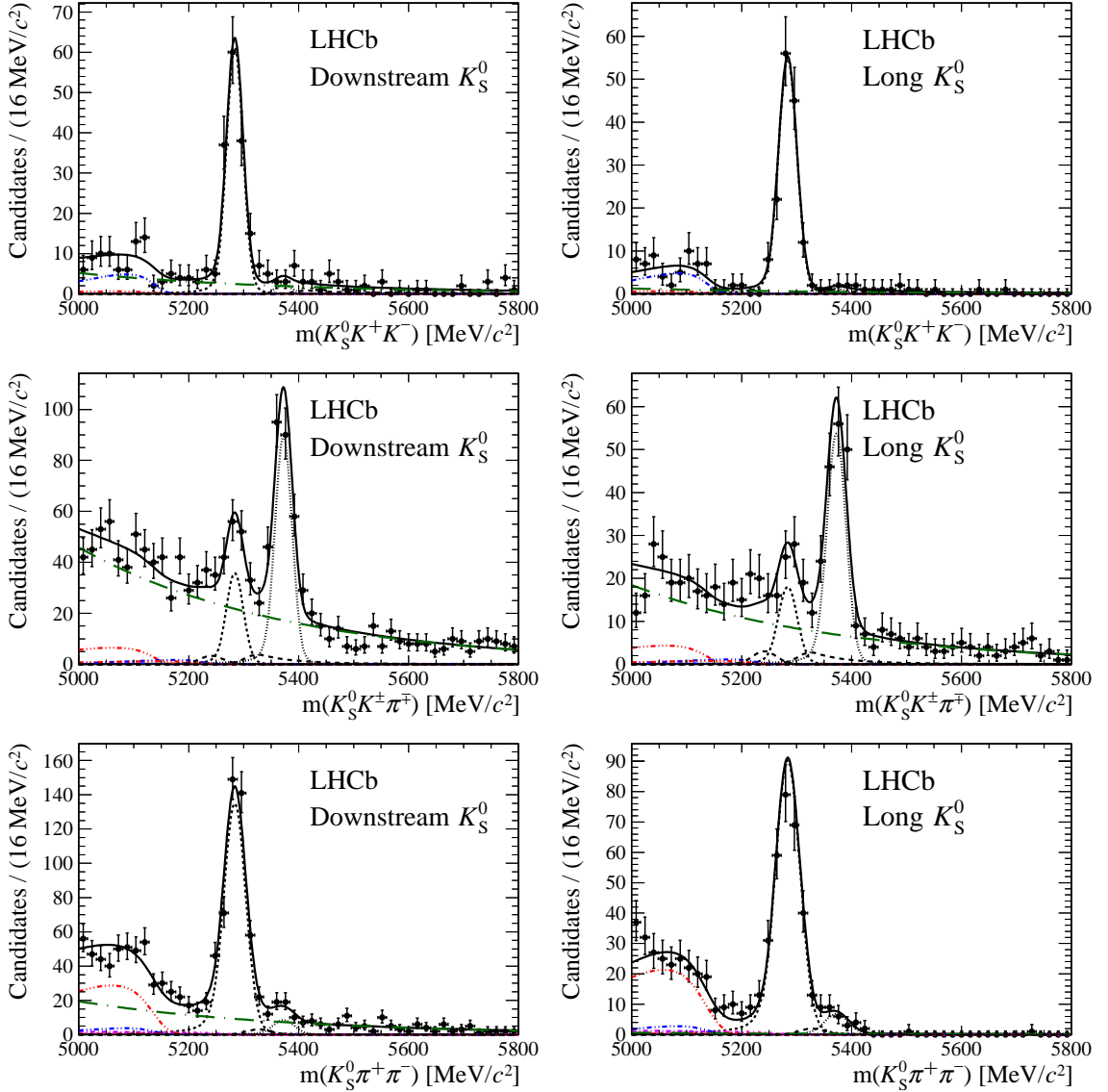


Figure 13: Invariant mass distributions of (top) $K_S^0 K^+ K^-$, (middle) $K_S^0 K^\pm \pi^\mp$, and (bottom) $K_S^0 \pi^+ \pi^-$ candidate events, with the tight selection for (left) Downstream and (right) Long K_S^0 reconstruction categories. In each plot, the total fit model is overlaid (solid black line) on the data points. The signal components are the black short-dashed or dotted lines, while cross-feed decays are the black dashed lines close to the signal peaks. The combinatorial background contribution is the green long-dash dotted line. Partially reconstructed contributions from various sources are also shown.

6 Summary

A review of recent results of the analyses of charmless three-body decays of b -hadrons has been presented. With the B -factories exploiting their final datasets and LHCb starting to analyse the 2fb^{-1} 2012 data sample there should be many more interesting results to come in the near future, both in B meson decays and in the almost completely unexplored territory of the decays of the Λ_b^0 and other b -baryons.

ACKNOWLEDGMENTS

Work supported by the European Research Council under FP7 and by the United Kingdom's Science and Technology Facilities Council.

References

- [1] R. Aaij *et al.* (LHCb Collaboration), Phys. Rev. Lett. **110**, 221601 (2013), arXiv:1304.6173 [hep-ex].
- [2] M. Gronau, Phys. Lett. B **492**, 297 (2000), hep-ph/0008292.
- [3] T. Latham and T. Gershon, J. Phys. G **36**, 025006 (2009), arXiv:0809.0872 [hep-ph].
- [4] A. Garmash *et al.* (Belle Collaboration), Phys. Rev. Lett. **96**, 251803 (2006), hep-ex/0512066.
- [5] B. Aubert *et al.* (BaBar Collaboration), Phys. Rev. D **78**, 012004 (2008), arXiv:0803.4451 [hep-ex].
- [6] J. P. Lees *et al.* (BaBar Collaboration), Phys. Rev. D **85**, 112010 (2012), arXiv:1201.5897 [hep-ex].
- [7] R. Aaij *et al.* (LHCb Collaboration), Phys. Rev. Lett. **111**, 101801 (2013), arXiv:1306.1246 [hep-ex].
- [8] A. A. Alves, Jr. *et al.* (LHCb Collaboration), JINST **3**, S08005 (2008).
- [9] J. Beringer *et al.* (Particle Data Group), Phys. Rev. D **86**, 010001 (2012).
- [10] J. P. Lees *et al.* (BaBar Collaboration), arXiv:1305.4218 [hep-ex].
- [11] R. Aaij *et al.* (LHCb Collaboration), LHCb-CONF-2012-028.

- [12] R. Aaij *et al.* (LHCb Collaboration), Phys. Rev. D **88**, 052015 (2013), arXiv:1307.6165 [hep-ex].
- [13] M. Pivk and F. R. Le Diberder, Nucl. Instrum. Meth. A **555**, 356 (2005), physics/0402083 [physics.data-an].
- [14] R. Aaij *et al.* (LHCb Collaboration), Eur. Phys. J. C **73**, 2462 (2013), arXiv:1303.7133 [hep-ex].
- [15] V. Gaur *et al.* (Belle Collaboration), Phys. Rev. D **87**, 091101 (2013), arXiv:1304.5312 [hep-ex].
- [16] A. E. Snyder and H. R. Quinn, Phys. Rev. D **48**, 2139 (1993).
- [17] J. P. Lees *et al.* (BaBar Collaboration), Phys. Rev. D **88**, 012003 (2013), arXiv:1304.3503 [hep-ex].
- [18] R. Aaij *et al.* [LHCb Collaboration], to appear in JHEP, arXiv:1307.7648 [hep-ex].
- [19] P. del Amo Sanchez *et al.* (BaBar Collaboration), Phys. Rev. D **82**, 031101 (2010), arXiv:1003.0640 [hep-ex].
- [20] R. Aaij *et al.* (LHCb Collaboration), JHEP **1304**, 001 (2013), arXiv:1301.5286 [hep-ex].